Journal of Petroleum Exploration and Production Technology
https://doi.org/10.1007/s13202-024-01772-0

ORIGINAL PAPER-PRODUCTION ENGINEERING

Upper limit estimate to wellhead flowing pressure and applicable gas production for a downhole throttling technique in high-pressure–high-temperature gas wells

Faqing Wang[1] · Deyou Qin[2] · Bao Zhang[1] · Jianfeng He[1] · Fangzhi Wang[1] · Ting Zhong[1] · Zhida Zhang[1]

Received: 18 June 2023 / Accepted: 16 February 2024

Abstract
In recent years, China has explored and exploited several high-pressure deep gas fields. Normally, high-pressure gas wells are gathered and processed through multichoke manifolds on well sites, creating hazards such as high wellhead flowing pressure (Pt) and high risk for on-site operation personnel. Moreover, downhole chokes have been used in place of surface chokes. In doing this, the Joule–Thomson (JT) effect is geothermally regulated, alleviating the formation of hydrates in surface facilities. However, its applicability to high-pressure gas wells is less explored. In an effort to guide its use, the objective of this study is to set selection criteria in terms of the allowable wellhead Pt and gas flow rate. First, isenthalpic lines are separately estimated for dry gas and high liquid hydrocarbon (LHC) content gas condensate at various inlet temperatures with the use of commercial software. Next, by analysis of the resulting isenthalpic curves, several results are obtained on the JT inversion curves and throttling process through a choke. Third, building on these insights, a method for projecting the maximum Pt is presented, leading to a value of 52.5 MPa. Finally, multiparameter models are separately run for two deep gas wells (8100 m and 5000 m), reinforcing the result of the pressure upper limit while maintaining a maximum daily gas production of 14 E4 m^3. Both upper limits with a maximum Pt of 52.5 MPa and daily gas production of 14 E4 m^3 are corroborated with field data records. These findings are vital to the selection of a viable high-pressure gas well for applying the downhole throttling technique.

Keywords High-pressure gas well · Downhole throttling · Joule–Thomson coefficient · Isenthalpic curve · Pressure drop · Temperature drop

List of symbols

- H Enthalpy (10^6 J)
- P Pressure (MPa)
- T Temperature (°C)
- U Internal energy (10^6 J)
- V Volume (m^3)
- μ_J Joule–Thomson coefficient (°C/MPa)

✉ Faqing Wang
wangfq-tlm@petrochina.com.cn; wangfaqing942@qq.com

[1] Oil & Gas Engineering Research Institute, Tarim Oilfield Company, PetroChina, Kuerle 841000, Xinjiang, China

[2] Yingmai Oil & Gas Development Division, Tarim Oilfield Company, PetroChina, Kuerle 841000, Xinjiang, China

Introduction

A high-pressure–high-temperature (HPHT) well designates a well condition of a formation pressure gradient above 18 kPa/m and reservoir temperature greater than 150 °C. It usually accompanies deep or ultradeep wells. In recent years, China has explored and exploited these onshore deep or ultradeep gas fields in the Sichuan, Tarim, and Ordos basins (Wu et al. 2020; Zhang and Emami-Meybodi 2020a; Zhu et al. 2021). During the early production of these HPHT gas wells, wellhead pressures are often excessively high, posing a high risk for on-site operation personnel. For the flowing well stream in the tubing, both the temperature and pressure of upwards-travelling gas gradually decrease. Under the conditions of critically low temperature and high pressure, natural gas is prone to hydrate formation; hydrates can block wellbores and/or pipelines (Ping et al. 2022; Sadeq et al. 2020, 2017; Wei et al. 2021). For safe operation, the hydrate formations need to be avoided. Therefore, either the

Published online: 22 March 2024

pressure needs to be reduced or the temperature of flowing gases needs to be increased (Bui et al. 2018; Gambelli and Rossi 2023; Kakitani et al. 2019; Marsetyo et al. 2023).

Downhole chokes are being used in lieu of surface heaters and methanol injection for the mitigation of gas hydrate formation in surface facilities. By moving the point of pressure and temperature reduction downhole, the Joule–Thomson (JT) effect across the choke is thermally regulated (Luo and Wu 2020; White et al. 2014). Downhole chokes are also extensively utilized to reduce wellhead pressures for high-pressured and/or ultrahigh-pressure gas wells (Jiang et al. 2015). This technique has compelling advantages compared to surface chokes. The latter requires more areas to accommodate surface manifold facilities, which often entail an accompanying heater to alleviate the hydrate formation and produce subsequent plugging problems with pipelines. A downhole choke is also a competitive choice in gas production for offshore applications, where the space is very limited to accommodate the manifolds and their corresponding auxiliaries (Bigdeli et al. 2023). In addition, it reduces the surface gathering pressure, with the intended aim of heating cooled gas downstream of chokes.

However, during the early exploitation of HPHT gas wells, the pressures downstream a choke remain high enough and result in an undesirable JT heating effect, even if a choke is moved underground. Hence, a maximum wellhead flowing pressure (Pt) must exist for an HPHT gas well for the placement of a downhole choke, ensuring a cooled downstream temperature. Moreover, deep or ultradeep wells have fairly high gas production to be economically viable. A higher gas flow rate correlated to a higher downstream temperature across a choke; this occurs to the extent that it exceeds the ambient temperature, as evidenced in the study by Li et al. (2012) and Jia et al. (2020). This is undesirable and negates the intended aim of harnessing geothermal energy. Therefore, an upper limit to gas production for HPHT gas wells also exists in the application of the downhole throttling technique.

Farzaneh-Gord et al. indicated that the GERG-2008 equation of state calculated the JT inversion curve with high accuracy and developed a novel correlation for its estimation (Farzaneh-Gord et al. 2020). Agwu et al. developed a critical review of extant models for modelling oil and gas flow rates through chokes (Agwu et al. 2022; Shao et al. 2018). Xie et al. proposed a comprehensive model for predicting the production of downhole choke wells (Xie et al. 2022). For gas flow rate prediction through wellhead chokes in gas condensate fields, robust hybrid machine learning algorithms (Abad et al. 2022) or vector machine algorithms (Nejatian et al. 2014) have been used. Moreover, as a long-established technology, the downhole throttling technique receives widespread acceptance, demonstrated by a wealth of scientific papers. Jiang et al. suggested its use in mitigating sustained casing pressure in an HPHT gas well (Jiang et al. 2015). White et al. showed its field applications and performance impact (White et al. 2014). Temperature prediction through chokes was performed for high-pressure gas/water/monoethylene glycol (MEG) mixtures (Jia et al. 2020), for HPHT gas condensates (Li et al. 2012), and in highly choked conditions (Teng et al. 2016). Multiphase choke performance prediction has also been improved (AlAjmi et al. 2015). However, to the best of our knowledge, few efforts have been reported in the literature regarding downhole throttling applicability in HPHT gas wells. In an effort to guide its utilization, the objective of this study is to set selection criteria by finding the maximum wellhead flowing pressure and gas flow rate upper limit, which are applicable for downhole throttling techniques in HPHT gas wells.

This paper, in relation to others, aims to address the following research gaps:

- The isenthalpic performances of both dry gas and high liquid hydrocarbon (LHC) content gas condensates are separately explored, and the pressures from both JT inversion curves are between 40 and 50 MPa.
- To utilize a downhole choke, the upper limit to the wellhead following pressure is 52.5 MPa. Otherwise, downhole throttling will exhibit an undesirable JT heating effect.
- To be geothermally viable for downhole throttling, the daily gas production needs to be less than 14 E4 m^3, as along with the preceding pressure limit.

This paper is organized as follows: First, a brief explanation is provided on the throttling process that occurs across downhole chokes. Next, the isenthalpic curves of both dry gas and high LHC content gas condensates are plotted to explore their respective isenthalpic characteristics, with temperature and pressure ranges covering field applications. Some intuitive observations are derived from both charts. Third, based on the above results, an applicability study on downhole throttling is performed. Finally, some important conclusions are drawn.

Throttling process in a nutshell

A throttling JT process is a thermodynamic process in which the enthalpy of the gas or the medium remains constant (Yarveicy et al. 2018). Enthalpy has the following defined expression (Li et al. 2012):

$$H = U + \mathrm{PV} \tag{1}$$

During the throttling process, no work is done by or on the system (dW = 0), as opposed to the turbine machinery, and usually no heat transfer occurs from or into the system (dQ = 0). Specifically, during the expansion (throttling) process, heat is not being evolved or absorbed. Thus, the process falls into an adiabatic process; specifically, no heat exchange occurs with the surroundings. In the end, the total energy balance reduces to the following (Teng et al. 2016):

$$\Delta H = 0 \tag{2}$$

For such a specialized case, no change in the system enthalpy is achieved. Therefore, the throttling process contains an isenthalpic process. However, the throttling process cannot be isentropic; it is a fundamentally irreversible process. The characteristics of the throttling process are as follows: 1. no work transfer; 2. no heat transfer; 3. irreversible process; 4. isenthalpic process.

A throttling of the flow causes a significant reduction in pressure because a throttling device causes a local pressure loss. A throttling process can be attained simply by introducing a restriction into a line through which a gas or liquid flows. This restriction is commonly performed by means of a partially open valve or a porous plug (see Fig. 1). During a throttling or JT process, a Joule–Thomson effect occurs, and its extent is quantified by the Joule–Thomson coefficient. The Joule–Thomson coefficient μ_J is the ratio of the temperature decrease to the pressure drop and has the following definition:

$$\mu_J = (\partial T/\partial P)_h \tag{3}$$

where T is the temperature, P is the pressure, and h is the enthalpy. For natural gas at low and intermediate pressures, μ_J >0 and $P_1 > P_2$; thus, the gas is cooled ($T_1 > T_2$) as it travels in a choke.

Isenthalpic curves of dry gas and gas condensate

Method of experimental measurement

The experiment to perform adiabatic throttling is known as the Joule–Thomson lab (Huang and Yang 2019; Jia et al. 2020; Zhu and Okuno 2015). In the setup represented schematically in Fig. 2(left), the inlet conditions are kept unchanged at position 1, the openness of the throttling unit is adjusted, and the different downstream states for 2a, 2b, 2c, and so on are measured. The pressures and temperatures related to various outlet conditions are recorded and plotted

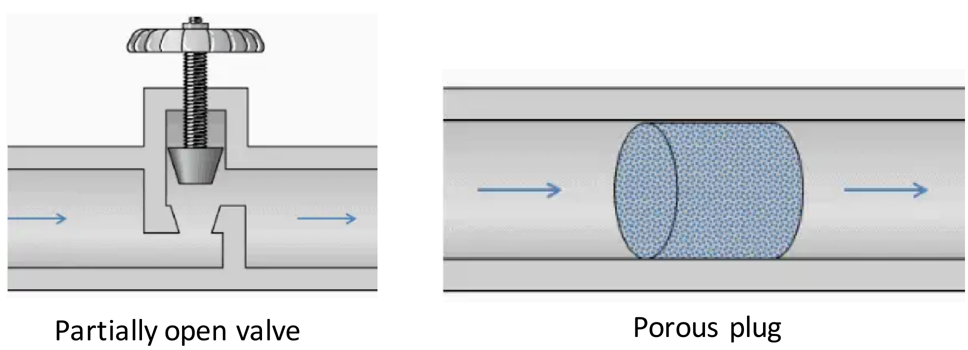

Fig. 1 Throttling processes in action

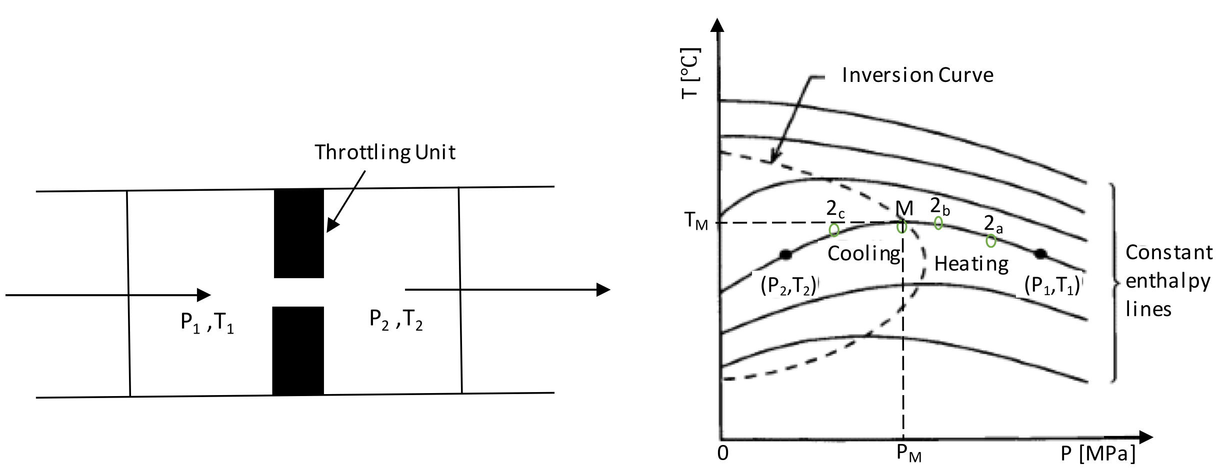

Fig. 2 Adiabatic throttling process (left), T–P diagram of a fluid (right)

on a T versus P diagram, as shown in Fig. 2(right). Since the upstream enthalpy is equal to the downstream enthalpy of the throttling unit, a large number of state points, such as 1, 2a, 2b, and 2c, has the same enthalpy. The line intersecting these points is thus isenthalpic. By shifting the pressure and/or temperature at position 1 and redoing the preceding experiments, another isenthalpic curve is achieved. Thus, a cluster of isenthalpic curves is created on a T–P plane.

Figure 2 (right) shows how pressure and temperature are related for a series of isenthalpic (Joule–Thomson) expansions. For example, if we start at point 1 (P_1, T_1) in the figure and the gas is throttled through a restriction, the pressure and temperature follow the isenthalpic line containing point 1. If the final pressure is P_2, then the final temperature will be $T_{2,}$ as shown by point 2 (P_2, T_2). Since the Joule–Thomson process is isenthalpic, the slope of each line can be represented as $(\delta T/\delta P)_h$. This quantity is referred to as the Joule–Thomson coefficient μ_{J}.

Figure 2 (right) shows that μ_{J} is negative at high pressures and high temperatures. Therefore, the gas heats up as it expands under these conditions. At lower temperatures, the temperature of the gas continues to increase if an expansion occurs at high pressures. However, at lower pressures, the slope, and hence μ_{J} becomes positive; thus, the gas cools upon expansion. The intermediate between these two effects is a pressure and temperature condition where $\mu_{\mathrm{J}} = 0$, as labelled point M in Fig. 2 (right). This temperature is known as the Joule–Thomson inversion temperature T_{M}, with the corresponding pressure P_{M} as the inversion pressure. Its value depends on the starting pressure and temperature and the nature of the gas.

The Joule–Thomson inversion curve is the locus in the T–P plane for which $\mu_J = 0$ (where the temperature is invariant upon isenthalpic expansion). Within the region bordered by the inversion curve, temperature decreases when pressure is reduced, resulting in a JT cooling effect ($\mu_{\mathrm{J}} > 0$). However, outside of this region, the expansion will result in a JT heating effect ($\mu_{\mathrm{J}} < 0$). This curve is important in refrigeration and liquefaction processes since the sign of the JT coefficient determines whether the temperature of a real gas rises or falls by isenthalpic expansion. The experimental measurement of the JT inversion curve needs the measurement of the volumetric or caloric properties under certain conditions; therefore, its accurate measurement is difficult (Farzaneh-Gord et al. 2020).

Method of equations of state calculation

Values of the Joule–Thomson coefficient can be obtained from equations of state. Many vigorous isenthalpic flash methods exist in the literature (Heidari et al. 2014; Huang and Yang 2019; Yarveicy et al. 2018; Zhu and Okuno 2015). Di Zhu et al. presented a robust isenthalpic flash for multiphase water-containing hydrocarbon mixtures. Desheng Huang et al. performed multiphase isenthalpic flash calculations for compound mixtures of water/solvent/hydrocarbon at high pressures and elevated temperatures. Heidari et al. (2014) developed a highly efficient method for thermal compositional simulators. In this work, the fluids examined are dry gas and high LHC content gas condensate; both are well studied, and hence, the use of commercial software to estimate their isenthalpic curves for various inlet temperatures is justified.

The multiphase flow models in the OLGA program (Bendlksen et al. 1991), a commercial software in widespread use, are utilized in this study to calculate temperatures downstream of a choke in an adiabatic setting. In the OLGA program setup shown in Fig. 3, both "P_In" and "P_Out" are the pressure nodes, with the user entering pressures for the inlet and outlet, respectively. With a flow path titled "FLOWPATH_1" that is 10 m long, a valve model on hydrovalve is placed in its middle. A self-explanatory option for temperature is selected as "ADIABATIC." A PVT table file is created with a third party software known as Multiflash and imported into this OLGA model, the compositions of which are listed in Table 1.

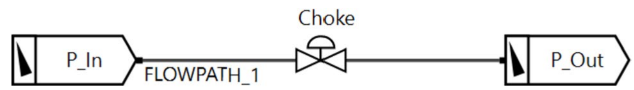

Fig. 3 OLGA program setup for the isenthalpic curve projections

Table 1 Compositions for the dry gas and high LHC content gas condensate

Component	Dry gas	Gas condensate
Carbon dioxide	0.7	1.572
Nitrogen	1.218	1.066
Methane	97.702	89.101
Ethane	0.346	2.340
Propane	0.021	0.630
Iso-Butane	0.002	0.138
N-Butane	0.005	0.209
Iso-Pentane	0.002	0.080
N-Pentane	0.002	0.099
Hexane	0.001	0.210
Heptane	0.001	0.275
Octane	0.0	0.575
Nonane	0.0	0.586
Decane	0.0	0.477
C11+	0.0	2.642

C11+ MW 230 g/mol, Density 0.8453 g/cm^3

Method of OLGA software simulation

The OLGA simulator is one of the principal components in the analysis of pipeline operations and well production optimizations (Bruijnen and de Boer 2016; Ganat et al. 2017; Zhang et al. 2023; Zhou et al. 2017). OLGA is a computational program developed to emulate multiphase flow in flow lines and pipeline networks, with processing equipment included. The program solves separate continuity equations for the gas, liquid bulk and liquid droplets: two momentum equations, one for the continuous liquid and one for the combination of gas and possible liquid droplets; and one mixture energy equation that considers that both phases are at the same temperatures. The equations are solved using the finite volume method and semi-implicit time integration. Successful designs and operations of multiphase production systems rely on a detailed understanding of flow behavior. OLGA provides a solution by accurately modelling true dynamics. Its transient simulator has an additional dimension to the traditional two-phase steady-state analysis by predicting the system dynamics, such as time-varying changes in flow rates, fluid composition, temperature, and operational shifts.

From wellbore dynamics for any well configuration to pipeline networks with many types of process equipment, the simulator engine provides an accurate prediction of the key operational conditions involving transient fluid flow (Bigdeli 2021; Bigdeli et al. 2019). After the model is set up as illustrated in Fig. 3, a table data file is created with the third party software Multiflash for dry gas (see Table 1 for its compositions) and imported to OLGA through the FILES keyword. Next, the steps below are followed:

(1) For “P_In”, the pressure node, an inlet temperature of 172 °C and inlet pressure of 98.8 MPa are entered.
(2) For “P_Out”, another pressure node, outlet temperature of 15 °C and pressure of 48.8 MPa at their respective box on the “Model Browser” are entered.
(3) The signs of “Ready to simulate” and a green circle on the bottom left of the main window dialog box are checked; this indicates that the model is ready to run.
(4) After the run is complete, the menu item “Profile Plot” is selected and the variables “PT” and “TM” are selected to display.
(5) On the resulting plot, the inputs of 98.8 MPa and 172 °C and the outputs of 48.8 MPa and 179.952 °C are selected and read.
(6) To obtain throttling temperatures other than 48.8 MPa, step 2 is used, and the pressure is changed.

Steps 2 through 6 are redone and an isenthalpic line of 172 °C in Fig. 4 is created. To obtain other lines, such as 158, 118, 78, 58, 38, and 18 °C, separately, steps 1 through 6 are repeatedly followed. Thus, the isenthalpic curves for dry gas at various inlet temperatures are obtained. With a high LHC content gas condensate, the preceding procedures are iterated for pressures from 2.54 MPa through 98.8 MPa, spanning a wide temperature range of 18 °C to 172 °C, and Fig. 5 is attained.

In either Figs. 4 or 5, the linking maxima from each isenthalpic curve form a line of the JT inversion curve, which falls between 40 and 50 MPa for both fluids at temperature ranges of 18 to 172 °C. The JT inversion curve is defined as the locus of the points where the JT coefficient becomes zero. It separates the region of positive JT coefficients from negative coefficients (Farzaneh-Gord et al. 2020). Nichita et al. calculated two typical reservoir fluids as examples, whose inversion pressures had a range of 35–50 MPa for typical reservoir temperatures (Nichita and Leibovici 2006). The JT inversion curve is important because it determines the sign of

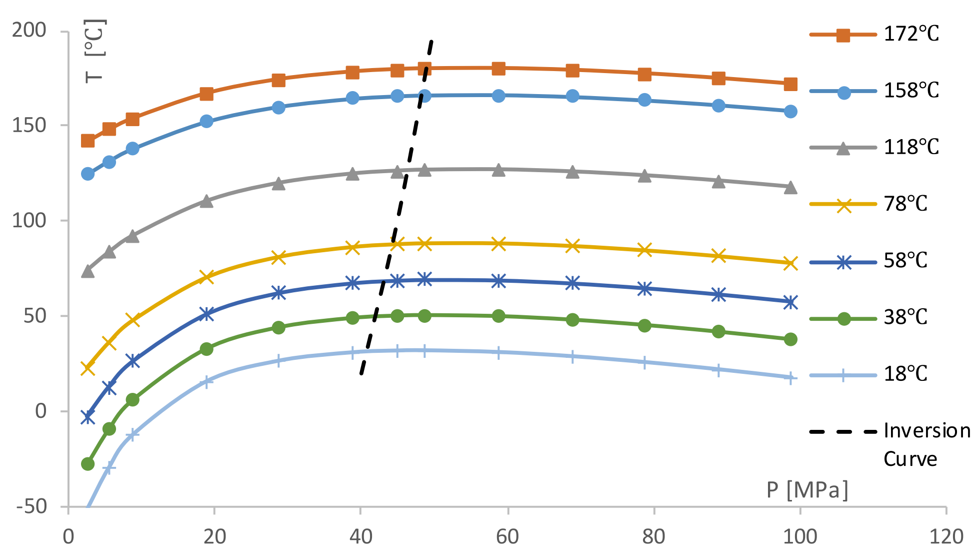

Fig. 4 Isenthalpic curves for dry gas at various inlet temperatures

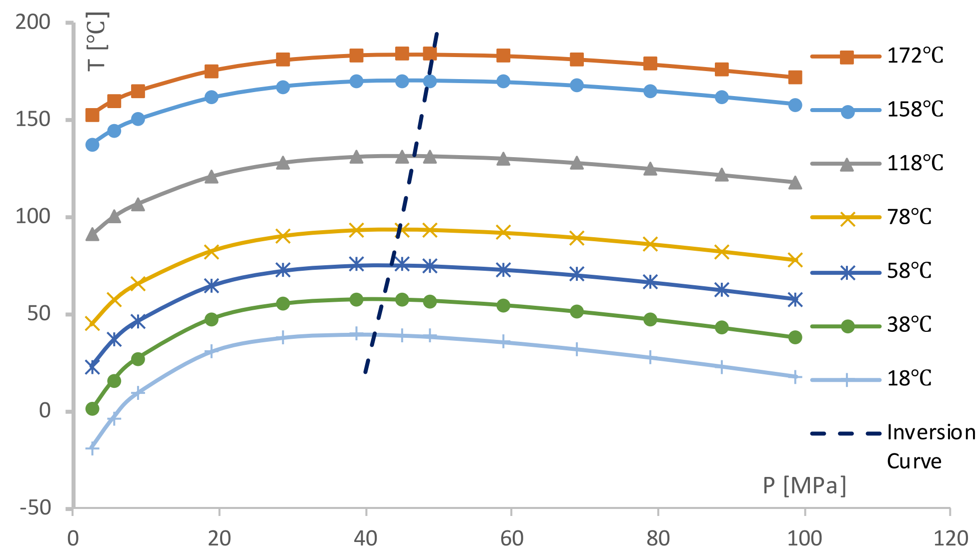

Fig. 5 Isenthalpic curves for high LHC content gas condensate at different inlet temperatures

the JT coefficient. To the right of these inversion curves, JT coefficients are negative (μ_J<0), which results in a JT heating effect; this means a hotter gas after the expansion of the choke. Moreover, on the left-hand side of both inversion curves, the signs of the JT coefficients are positive, exposing the gas or condensate gas to a JT cooling effect. At the locus of these inversion curves, their JT coefficients are zero. Evidently, only points traversing inversions can have an invariant temperature during throttling processes.

By analyzing both Figs. 4 and 5, the following can be observed: ① For pressures above 28.8 MPa, all isenthalpic curves from different inlet temperatures are nearly flat. This indicates that downhole throttling is inapplicable for pressures higher than 28.8 MPa. Had downhole throttling occurred at pressures above 28.8 MPa, it will encounter an increase in temperature as pressure is reduced across a choke. This can contradict the aim of exploiting the geothermal energy. ② When the inlet temperature is above a certain value, the temperatures downstream of the choke are higher than the ambient temperature at the location of the downhole choke. Therefore, downhole chokes are applicable solely for low-production gas wells. This is partly because positive JT coefficients occur in the low inlet temperature region of both charts. Furthermore, low inlet temperatures entails low gas flow rates. On the other hand, for a gas with a high enough inlet temperature, its cooled downstream temperature through a choke is still high, to the extent above ambient.

Applicability study on downhole throttling

Determination of maximum Pt

Based on preceding insights that downhole throttling is not suitable for downstream pressures higher than 28.8 MPa, the objective of this study is to find its corresponding Pt, which is also the maximum allowable wellhead pressure for economically installing downhole chokes. We make a point of effectively absorbing geothermal energy by cooled gas streams. To determine this value, the following three conventions are used:

1. On depth at which downhole chokes are placed, we review 69 downhole choke installations that have been deployed in our oil field since June 2011. Its seating depth scatter chart is shown in Fig. 6. Integrating it with applications in other oil fields in China, we find a preferred depth of 2500 m. By the same means, we obtain a roughly accepted wellhead flowing temperature of 28 °C on most downhole choke installations.
2. The allowable pressure drop that downhole chokes can endure has been widely accepted to be 35 MPa (Huiyun et al. 2020); this correlates to 30 MPa after factoring in a safety allowance of 0.85. The well site back pressure, which is also called the wellhead downstream pressure, is usually set at 10 MPa for gas gathering systems. The geothermal temperature is 65.05 °C in our oil field, corresponding to a downhole choke placement depth of 2500 m.
3. For the critical pressure ratio, a value of 0.546 is selected after performing a literature review (Huiyun et al. 2020; Jia et al. 2020; Naseri et al. 2016; Shao et al. 2018; Xie et al. 2022).

Assuming a choke is set at 2500 m downhole, a computing flow diagram, as illustrated in Fig. 7(left), is framed. The first step is entering an initial wellhead pressure of 80 MPa, and then, this flow chart is followed; a maximum pressure of 52.5 MPa is reached after multiple iterations. Specifically, if the wellhead flowing pressure is below this

Fig. 6 Scatter chart of the downhole choke depth versus the choke size in a western China field

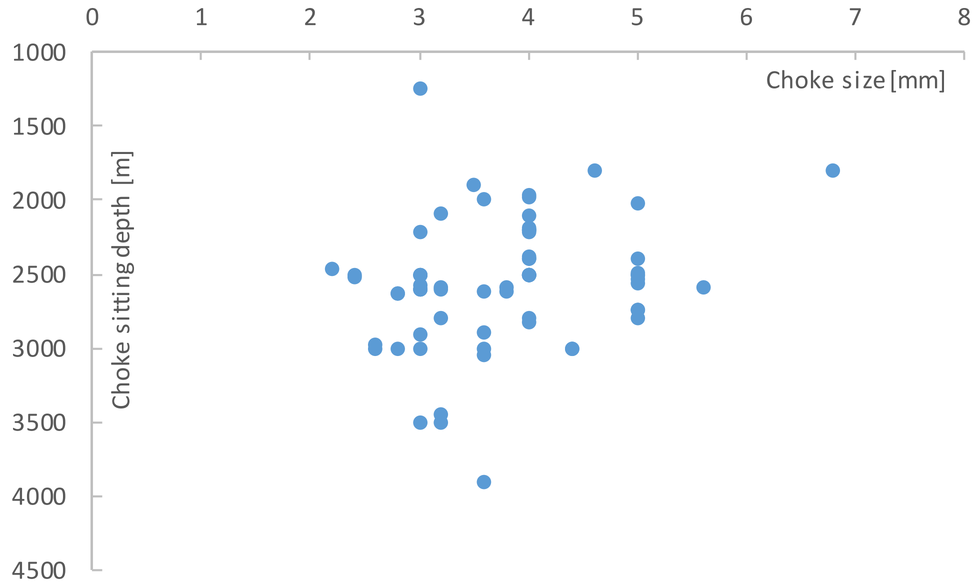

value, then a cooled gas is achieved downstream of the choke.

However, even if Pt is less than 52.5 MPa, the resulting cooled gas temperatures can still be higher than the ambient temperature of 65.05 °C if gas production is high enough. This negates our fundamental objective of having downhole throttling techniques, i.e., harnessing geothermal energy to heat chilled gas. To illustrate this phenomenon, data from Zhu Guangyou et al. are drawn on (Zhu et al. 2021), with key parameters listed in Table 2. A wellbore temperature profile is plotted in Fig. 7(right) for a wellhead flow pressure of 52.2 MPa, gas production being 15 E4 m^3/d. From this chart, even if the downstream temperature is lowered somewhat, it can still stand above the ambient line. Hence, suitable gas production is needed for a cooled gas through a choke to be geothermally heated.

Fig. 7 Flow diagram for estimating the maximum Pt (left) and the temperature profile for a wellhead flowing pressure of 52.2 MPa and gas production of 15 E4 m^3/d (right)

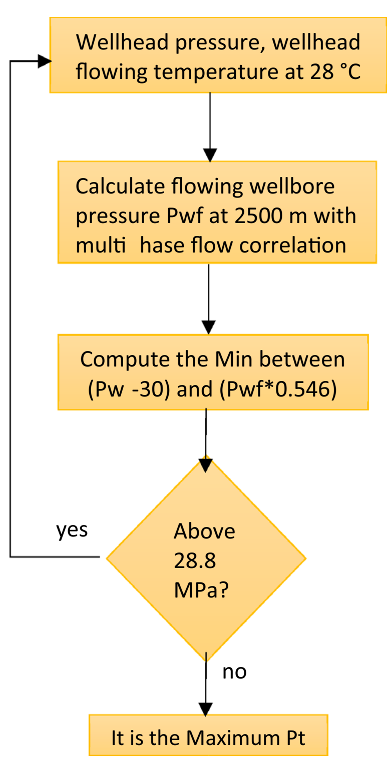

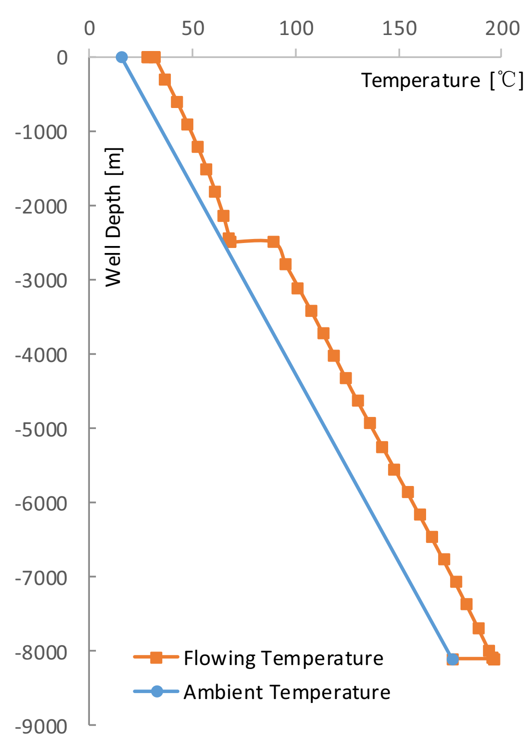

Table 2 Essential well parameters in use with a downhole choke

Parameters	Value	Parameters	Value
Diameter of tubing	φ88.9 × 6.45 mm	Diameter of casing	φ177.8 × 12.65 mm
Length of tubing	8080 m	Casing depth range	0–8100 m
Packer fluid viscosity	28 mPa s	Packer depth	8000 m
Packer fluid weight	1.7 g/cm^3	Geothermal gradient	1.98 ℃/100 m
Reservoir pressure	138 MPa	Wellhead temperature	15.55 ℃
Reservoir temperature	175.93 ℃	Gas specific gravity	0.64
Liquid gas ratio	0 m^3/m^3	Water cut	0

Table 3 Key variables used in the multi-case studies of the 8100 m well depth

Flowing Pt (MPa)	Reservoir pressure (MPa)	Pressure gradient (MPa/100 m)	Gas productivity index [E6 m^3/(d bar^2)]
52.5	138	1.70	1.124 E−7
	120	1.48	1.725 E−7
	80.8	1.00	1.993 E−6
25.8	138	1.70	8.692 E−8
	120	1.48	1.190 E−7
	80.8	1.00	3.182 E−7
	50.8	0.63	1.959 E−6

Applicable gas production

Gas stream temperatures in the downstream chokes are reliant on both upstream pressures and temperatures and throttling pressure drops. Upstream gas stream temperatures are a function of the gas flow rate and temperature gradients where a gas well is located and its well depth. To explore the gas production applicable to the downhole throttling technique, a vertical gas well in western China, which has an ambient temperature gradient of 1.98 °C/100 m and a total vertical depth of 8100 m, was used. Other key parameters are listed in Table 2. The well stream used is dry gas, and its composition is listed in Table 1. The software utilized is commercially available and marketed as PIPESIM. In addition to a downhole choke deployed at 2500 m, a variable choke is installed at the Christmas tree, with the goal of safeguarding surface facilities in case of failures in the downhole choke. The outlet pressure is fixed at 10 MPa. To run multiple cases, other key variables are listed in Table 3, such as reservoir pressures and gas productivity indices (Kalantari-asl et al. 2022; Zhang and Emami-Meybodi 2020b).

After entering into or choosing from an appropriate amount of data in the PIPESIM graphic user interface, the allowable pressure difference through downhole choke is maintained by varying the beam size of the chokes for either downholes or surface chokes. Then, multiple runs are performed for various reservoir pressure gradients and gas productivity indices, simulating diverse well conditions. Therefore, Fig. 8 shows the resulting data. In this chart, two flowing Pts, at 52.5 MPa and 25.8 MPa, are separately provided. In Fig. 8 (left) for flowing Pt at 52.5 MPa, the subcooling remains above zero for all daily gas productions, and especially as low as 2.0 E4 m^3. This supports the results above, with a maximum wellhead flowing pressure of 52.5 MPa, as estimated from the flow diagram.

In Fig. 8 (right) for flowing Pt at 25.8 MPa, for the daily gas production below 14 E4 m^3, most subcooling is less than zero. Thus, from an engineering application viewpoint, that value is the applicable upper limit in the gas production to the downhole throttling technique. The subcooling values above zero are caused by a downhole throttling pressure drop constraint of 30 MPa. This also imposes an impact on the lower end of the line with pressure gradient 1.00 MPa/100 m. For the rest of the lines in Fig. 8(right), a lower gas flow rate correlate to a larger subcooling. Specifically, a larger temperature difference between the downstream and ambient conditions provides better benefits in the application of the downhole throttling technique.

To improve the robustness of the upshots above, another HPHT gas well with a typical well configuration is set up in PIPESIM. It is differentiated from the preceding example well with a well depth of 5000 m and the other information listed in Table 4.

After performing multiple cases with various reservoir pressures and gas productivity indices, Fig. 9 is obtained by visualizing the resultant data.

Both charts in Fig. 9 reinforce the findings from Fig. 8, with the exception of the applicable daily gas production being 16 E4 m^3. As the research target of this work is ultradeep wells, the preceding value is more desirable.

Statistical analysis of field applications

The downhole throttling technique has been deployed in a western China field for over a decade. In field applications, the maximum pressure drop across the downhole choke follows. In this work, data pairs of daily gas production and flowing Pt are shown in Fig. 10. The formation of pressure gradients, correlating to these datasets, span a range of 1.33–0.73 MPa/100 m. For this chart, both upper limits to

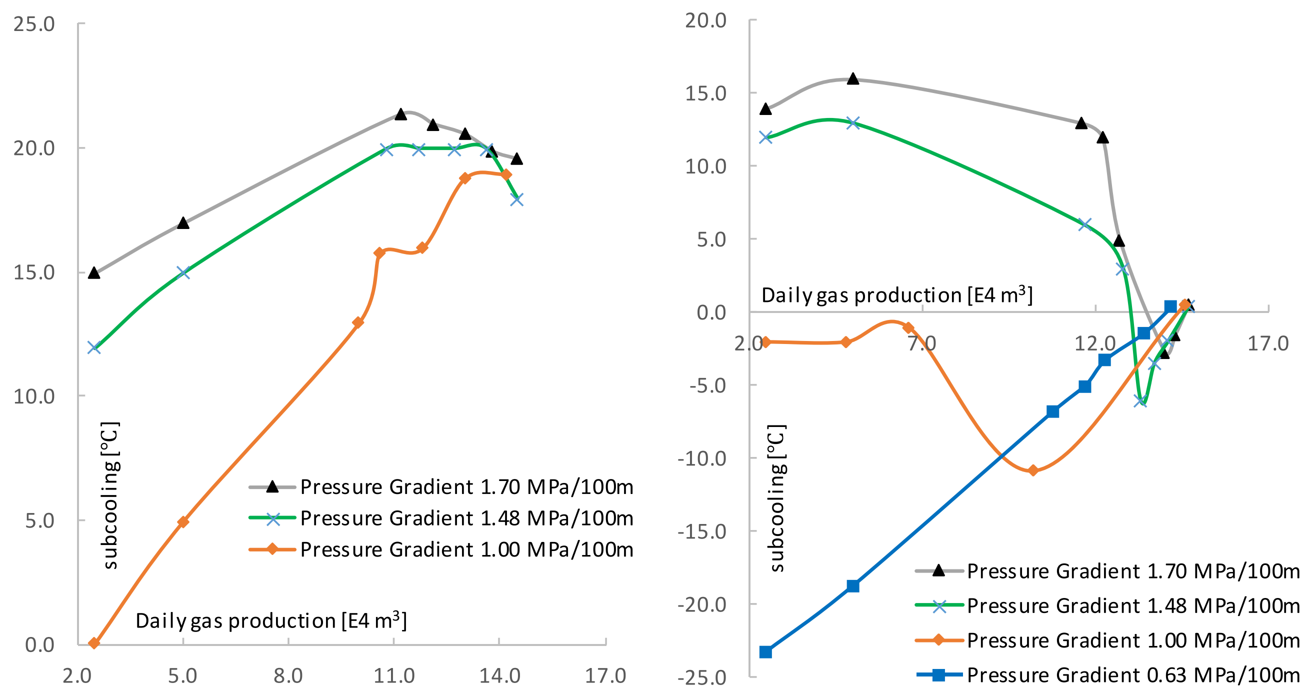

Fig. 8 Relationship between the daily gas production and subcooling at various formation pressure gradients for an 8100 m well depth with a constant flowing Pt at 52.5 MPa (left) and at 25.8 MPa (right). The subcooling is calculated by subtracting the ambient temperature at 2500 m from the downstream temperature

Table 4 Primary variables used in the multi-case studies of 5000 m well depth

Flowing Pt (MPa)	Reservoir pressure (MPa)	Pressure gradient (MPa/100 m)	Gas productivity index [E6 m^3/(d bar^2)]
52.5	85.0	1.70	5.826 E−7
	74.0	1.48	1.807 E−6
	69.0	1.38	1.508 E−5
25.8	64.0	1.28	5.501 E−7
	44.0	0.88	2.699 E−6
	38.5	0.77	1.649 E−5

the flowing Pt of 52.5 MPa and the daily gas production of 14 E4 m^3 are verified.

Downhole throttling application in action

To facilitate the use of the conclusions from this work, Fig. 11 is proposed as a simple decision tree. First, production engineers are expected to determine two inputs. One is flowing Pt, preferably at daily gas production as close to 14 E4 m^3 as possible. This is the flowing wellhead pressure before a downhole choke is deployed, and it is often available from well testing. The other is gas production, which is the desired gas flow rate after placing a downhole choke.

Discussion

This study has the following advantages and disadvantages.

Advantages: Isenthalpic lines of both dry gas and LHC content gas condensate are used to arrive at the pressure upper limit. Building on two deep gas gushers, multiple simulations are run and field data records are used to justify both upper limits of flowing Pt and gas production.

Disadvantages: The flowing upper pressure limit is based on practice; here, the allowable pressure difference through a downhole choke is 30 MPa. As technology advances, this constraint is likely to lessen. The upper gas production limit rests on a well site back pressure of 10 MPa, which is derived from the gas gathering system pressure. Since gas zones may mark major oil formations, their production needs lower well site back pressure.

Conclusions

First, a pair of T–P plots for dry gas and high liquid hydrocarbon (LHC) content gas condensates were separately calculated using commercial software. Second, a method to estimate the maximum wellhead flowing pressure (Pt) was proposed, and its exact value was determined with the application of downhole throttling. Third, based on the well data from two deep gas producers in western China,

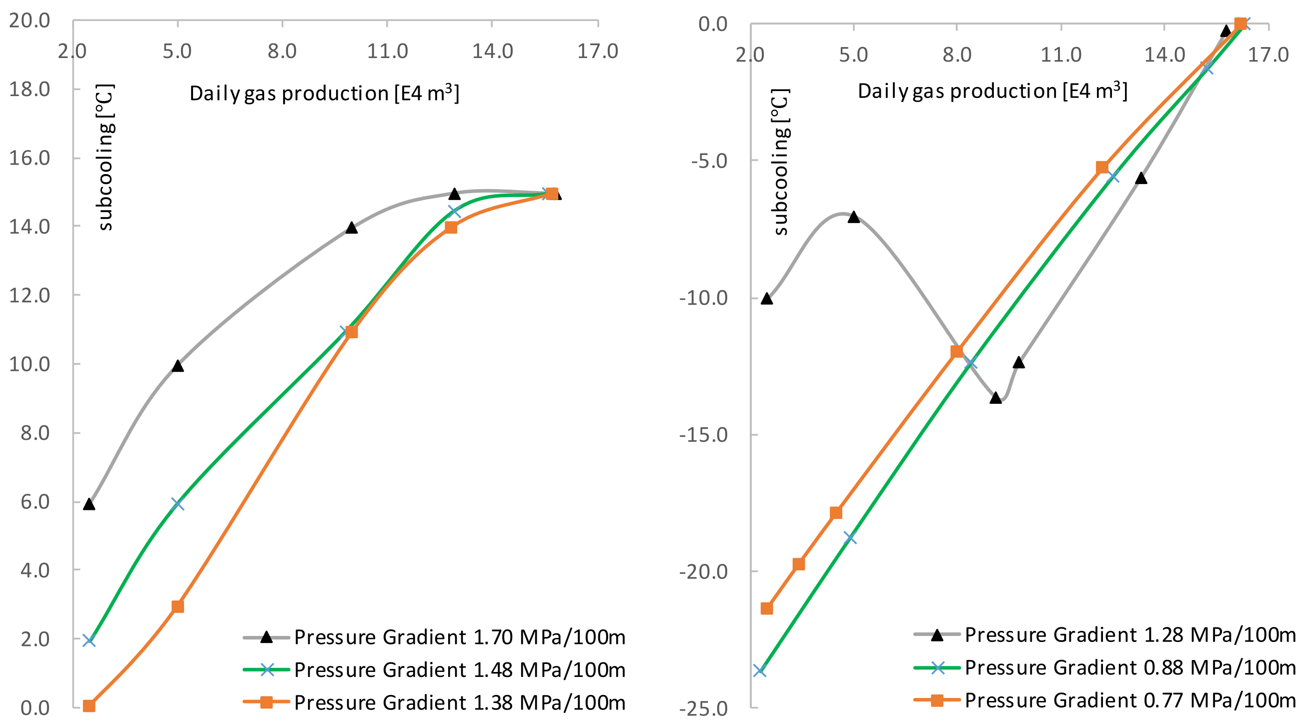

Fig. 9 Relationship between the daily gas production and subcooling at various formation pressure gradients for 5000 m well depth, with constant flowing Pt at 52.5 MPa (left) and at 25.8 MPa (right)

Fig. 10 Cross chart of the daily gas production versus flowing Pt

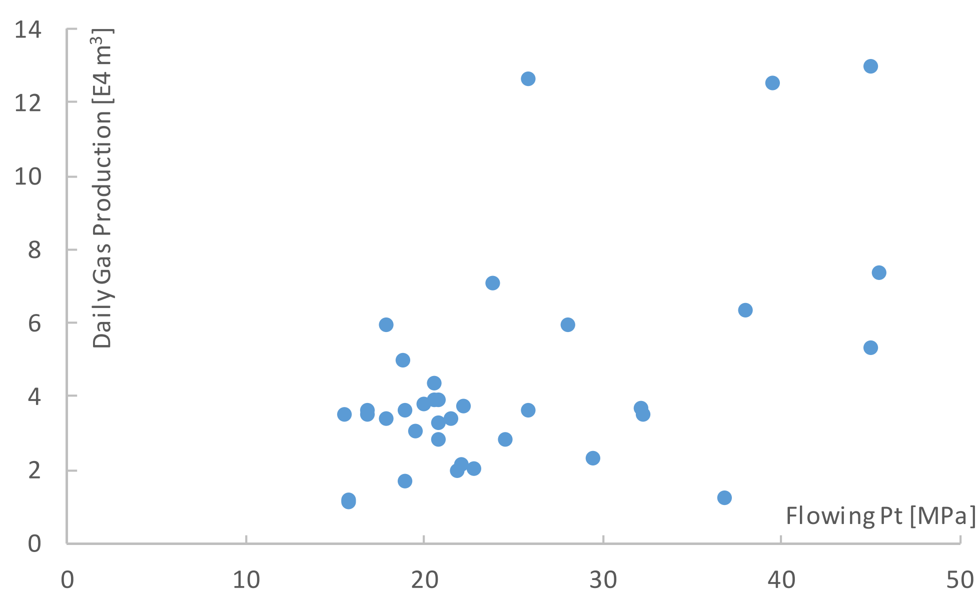

the pressure upper limit applicable to the downhole throttling technique was re-confirmed while separating the allowable maximum gas flow rate by running multiparameter modelling. Last, both upper limits were re-verified by statistical analysis of field data records. As such, the following conclusions were drawn:

1. The pressure upper limit for the downhole throttling technique was estimated to be 52.5 MPa. Otherwise, a hotter gas was encountered downstream of the chokes; this was indicative of a Joule–Thomson (JT) heating effect and an undesirable effect.

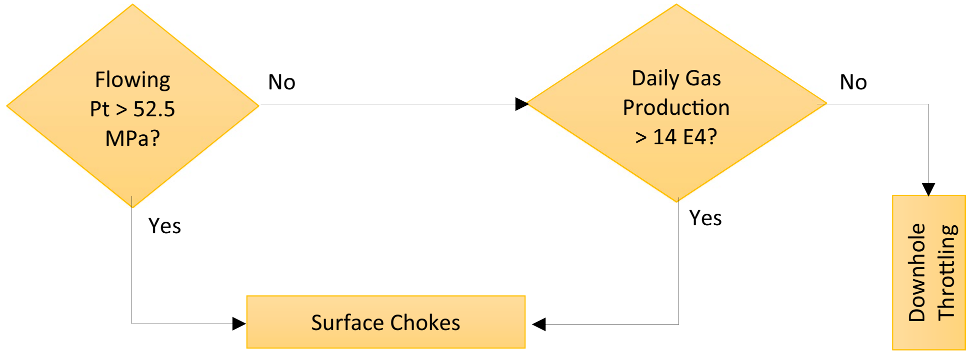

Fig. 11 Simple decision tree for selecting the downhole throttling or surface chokes

2. The pressure upper limit and the gas flow rate were important parameters. Daily gas production applicable to the downhole throttling technique was determined to be 14 E4 m^3. For the low formation pressure gradients, a lower gas flow rate correlated to a better gain of the JT cooling effect on downhole throttling.
3. The pressures of JT inversion curves of both dry gas and high LHC content gas condensate fell between 40 and 50 MPa at temperature ranges of 18–172 °C; this had implications in refrigeration and liquefaction processes.

Declarations

Conflict of interest The authors declare that they have no known competing financial interests or personal relationships that could have appeared to influence the work reported in this paper.

References

Abad ARB, Ghorbani H, Mohamadian N et al (2022) Robust hybrid machine learning algorithms for gas flow rates prediction through wellhead chokes in gas condensate fields. Fuel 308:121872. https://doi.org/10.1016/j.fuel.2021.121872

Agwu OE, Okoro EE, Sanni SE (2022) Modelling oil and gas flow rate through chokes: a critical review of extant models. J Petrol Sci Eng 208:109775. https://doi.org/10.1016/j.petrol.2021.109775

AlAjmi MD, Alarifi SA, Mahsoon AH (2015) Improving multiphase choke performance prediction and well production test validation using artificial intelligence: a new milestone. In: SPE digital energy conference and exhibition, Spe-173394-ms

Bendlksen KH, Malnes D, Moe R et al (1991) The dynamic two-fluid model OLGA: theory and application. SPE Prod Eng 6(02):171–180. https://doi.org/10.2118/19451-pa

Bigdeli A, Lima IDCM, Sepehrnoori K et al. (2019) Development of a novel framework for sequential coupling of reservoir, wells, and surface facilities. In: CILAMCE 2019 Proceedings of the XL Ibero-Latin-American Congress on Computational Methods in Engineering, ABMEC Natal/RN, Brazil, November 11–14. http://repositorio.ufc.br/handle/riufc/61727

Bigdeli A, von Hohendorff Filho JC,Schiozer DJ. (2023) Effect of liquid-liquid subsea separation on production forecast considering integration of a deepwater reservoir and surface facility models. In: SPE EuropEC - Europe energy conference featured at the 84th EAGE annual conference & exhibition, Vienna, Austria, 5–8 June https://doi.org/10.2118/214455-ms

Bigdeli A (2021) Sequential explicit and implicit coupling of 3D compositional reservoir, wells and surface facility. Ph.D, Chemical engineering, Federal University of Ceará. http://repositorio.ufc.br/handle/riufc/65269

Bruijnen PM, de Boer JP (2016) How to diagnose and solve a tripping ESP caused by multiphase flow behavior in a horizontal well. In: SPE middle east artificial lift conference and exhibition, Manama, Kingdom of Bahrain, November 30–December 1, https://doi.org/10.2118/184216-ms

Bui T, Sicard F, Monteiro D et al (2018) Antiagglomerants affect gas hydrate growth. J Phys Chem Lett 9(12):3491–3496. https://doi.org/10.1021/acs.jpclett.8b01180

Farzaneh-Gord M, Reza Rahbari H, Zangeneh J (2020) Effects of natural gas compositions on its Joule-Thomson coefficients and Joule-Thomson inversion curves. Cryogenics 111:103169. https://doi.org/10.1016/j.cryogenics.2020.103169

Gambelli AM, Rossi F (2023) Review on the usage of small-chain hydrocarbons (C_2—C_4) as aid gases for improving the efficiency of hydrate-based technologies. Energies 16(8):3576. https://doi.org/10.3390/en16083576

Ganat TA, Hrairi M, Hawlader MNA (2017) Validation of ESP oil wells measured parameters using simulation OLGA software. IOP Conf Series: Mater Sci Eng 184:012057. https://doi.org/10.1088/1757-899x/184/1/012057

Heidari M, Nghiem LX,Maini BB (2014). Improved isenthalpic multiphase flash calculations for thermal compositional simulators. In: SPE heavy oil conference-Canada https://doi.org/10.2118/170029-ms

Huang D, Yang D (2019) A robust multiphase isenthalpic flash model for water/solvent/hydrocarbon systems at high pressures and elevated temperatures. Fluid Phase Equilib 489:48–66. https://doi.org/10.1016/j.fluid.2019.02.005

Huiyun M, Yuan J, Qiang Y et al (2020) Optimum design of downhole chokes with high sulfur content and large pressure difference. IOP Conf Series: Earth Environ Sci 461(1):012043. https://doi.org/10.1088/1755-1315/461/1/012043

Jia W, Yang F, Wu X et al (2020) Predictions on temperatures of high-pressure gas/water/MEG mixtures flowing through wellhead chokes. J Nat Gas Sci Eng 74:103108. https://doi.org/10.1016/j.jngse.2019.103108

Jiang L, Xu H, Shi T et al (2015) Downhole multistage choke technology to reduce sustained casing pressure in a HPHT gas well. J Nat Gas Sci Eng 26:992–998. https://doi.org/10.1016/j.jngse.2015.07.026

Kakitani C, Marques DC, Marcelino Neto MA et al (2019) Measurements of hydrate formation behavior in shut-in and restart conditions. Energy Fuels 33(10):9457–9465. https://doi.org/10.1021/acs.energyfuels.9b01395

Kalantariasl A, Farhadi I, Farzani S et al (2022) A new comprehensive dimensionless inflow performance relationship for gas wells. J Petrol Explorat Prod Technol 12(8):2257–2269. https://doi.org/10.1007/s13202-022-01457-6

Li C, Jia W, Wu X (2012) Temperature prediction for high pressure high temperature condensate gas flow through chokes. Energies 5(3):670–682. https://doi.org/10.3390/en5030670

Luo W, Wu Q (2020) Development of wellbore compound blockage removal technology to reduce production loss in the ultra-deep and high-sulfur Yuanba gas field. J Petrol Explorat Prod Technol 10(8):3711–3721. https://doi.org/10.1007/s13202-020-01000-5

Marsetyo MM, Suranto, Herianto et al. (2023) Study of hydrate formation due to the Joule Thomson effect and optimization of methanol (MeOH) injection as a hydrate prevention method. In: 4th International conference on earth science, mineral and energy. https://doi.org/10.1063/5.0126565

Naseri S, Tatar A, Shokrollahi A (2016) Development of an accurate method to prognosticate choke flow coefficients for natural gas flow through nozzle and orifice type chokes. Flow Meas Instrum 48:1–7. https://doi.org/10.1016/j.flowmeasinst.2015.12.003

Nejatian I, Kanani M, Arabloo M et al (2014) Prediction of natural gas flow through chokes using support vector machine algorithm. J Nat Gas Sci Eng 18:155–163. https://doi.org/10.1016/j.jngse.2014.02.008

Nichita DV, Leibovici CF (2006) Calculation of Joule-Thomson inversion curves for two-phase mixtures. Fluid Phase Equilib 246(1):167–176. https://doi.org/10.1016/j.fluid.2006.05.025

Ping X, Han G, Cen X et al. (2022). Prediction of pressure and temperature profiles and hydrate formation region in ESP-lifted natural gas hydrate wells. In: SPE western regional meeting https://doi.org/10.2118/209288-ms

Sadeq D, Iglauer S, Lebedev M et al (2017) Experimental determination of hydrate phase equilibrium for different gas mixtures containing methane, carbon dioxide and nitrogen with motor current measurements. J Nat Gas Sci Eng 38:59–73. https://doi.org/10.1016/j.jngse.2016.12.025

Sadeq D, Al-Fatlawi O, Iglauer S et al. (2020) Hydrate equilibrium model for gas mixtures containing methane, nitrogen and carbon dioxide. In: Offshore technology conference, Houston, TX, USA, 4–7 May https://doi.org/10.4043/30586-ms

Shao H, Jiang L, Liu L et al (2018) Modeling of multiphase flow through chokes. Flow Meas Instrum 60:44–50. https://doi.org/10.1016/j.flowmeasinst.2018.02.015

Teng L, Zhang D, Li Y et al (2016) Multiphase mixture model to predict temperature drop in highly choked conditions in CO_2 enhanced oil recovery. Appl Therm Eng 108:670–679. https://doi.org/10.1016/j.applthermaleng.2016.07.156

Wei N, Jiang L, Zhao J et al (2021) Risk prediction of non-equilibrium formation of natural gas hydrate in the wellbore of a marine gas/water-producing well. Nat Gas Ind B 8(1):88–97. https://doi.org/10.1016/j.ngib.2020.07.005

White AJ, Lavery PE,Rock L (2014) Downhole choke applications and performance impact: a tupper field montney evaluation. In: SPE/CSUR unconventional resources conference – Canada, October 01–03 https://doi.org/10.2118/171598-ms

Wu X, Wan F, Chen Z et al (2020) Drilling and completion technologies for deep carbonate rocks in the Sichuan Basin: practices and prospects. Nat Gas Ind B 7(5):547–556. https://doi.org/10.1016/j.ngib.2020.09.012

Xie C, Liu Y, Li X et al (2022) A novel comprehensive model for predicting production of downhole choke wells. Fuel 313:122944. https://doi.org/10.1016/j.fuel.2021.122944

Yarveicy H, Ghiasi MM, Mohammadi AH (2018) Determination of the gas hydrate formation limits to isenthalpic Joule-Thomson expansions. Chem Eng Res Des 132:208–214. https://doi.org/10.1016/j.cherd.2017.12.046

Zhang F, Emami-Meybodi H (2020a) Flowback fracture closure of multi-fractured horizontal wells in shale gas reservoirs. J Petrol Sci Eng 186:106711. https://doi.org/10.1016/j.petrol.2019.106711

Zhang F, Emami-Meybodi H (2020b) A semianalytical method for two-phase flowback rate-transient analysis in shale gas reservoirs. SPE J 25(4):1599–1622. https://doi.org/10.2118/201225-pa

Zhang F, Zou L, Rui Z et al (2023) A two-phase type-curve method with multiscale fluid transport mechanisms in hydraulically fractured shale reservoirs. Pet Sci 20(4):2253–2267. https://doi.org/10.1016/j.petsci.2023.02.004

Zhou Y, Li X, Wojtanowicz AK et al. (2017) Multidimensional evaluation for safe and efficient killing using dynamic kill method: a case analysis in China. In: Abu Dhabi international petroleum exhibition & conference, Abu Dhabi, UAE, November 13–16, 2017 https://doi.org/10.2118/188636-ms

Zhu D, Okuno R (2015) Robust isenthalpic flash for multiphase water/hydrocarbon mixtures. SPE J 20(6):1350–1365. https://doi.org/10.2118/170092-pa

Zhu G, Milkov AV, Li J et al (2021) Deepest oil in Asia: Characteristics of petroleum system in the Tarim basin, China. J Petrol Sci Eng 199:108246. https://doi.org/10.1016/j.petrol.2020.108246